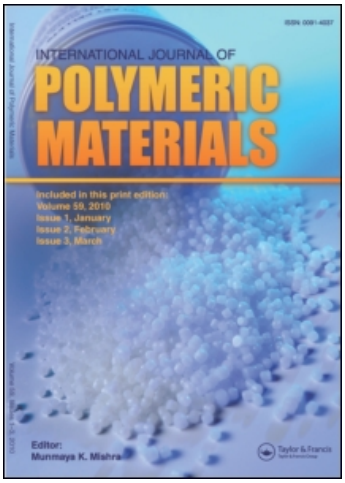

International Journal of Polymeric Materials
Publication details, including instructions for authors and subscription information:
http://www.informaworld.com/smpp/title~content=t713647664

POLY(ETHYLENE TEREPHTALATE)-CONTAINING POLYMER LIQUID CRYSTALS AND THEIR BLENDS

Witold Brostow; Magdalena Jaklewicz; Pablo Montemartini

Online publication date: 18 June 2010

To cite this Article Brostow, Witold , Jaklewicz, Magdalena and Montemartini, Pablo(2003) 'POLY(ETHYLENE TEREPHTALATE)-CONTAINING POLYMER LIQUID CRYSTALS AND THEIR BLENDS', International Journal of Polymeric Materials, 52: 11, 999 — 1034
To link to this Article: DOI: 10.1080/714975876
URL: http://dx.doi.org/10.1080/714975876

International Journal of Polymeric Materials, 52:999–1034, 2003

ISSN: 0091-4037 print/1543-5253 online
DOI: 10.1080/00914030390256882

Taylor & Francis
Taylor & Francis Group

POLY(ETHYLENE TEREPHTALATE)-CONTAINING POLYMER LIQUID CRYSTALS AND THEIR BLENDS

Witold Brostow
Laboratory of Advanced Polymers and Optimized Materials,
Department of Materials Science and Engineering,
University of North Texas, Denton, Texas, USA

Magdalena Jaklewicz
Laboratory of Advanced Polymers and Optimized Materials,
Department of Materials Science and Engineering,
University of North Texas, Denton, Texas, USA and
Department of Mechanical and Biomechanical Engineering,
Cracow University of Technology, Cracow, Poland

Pablo Montemartini
Laboratory of Advanced Polymers and Optimized Materials,
Department of Materials Science and Engineering,
University of North Texas, Denton, Texas, USA and
Consejo Nacional de Investigaciones Cientificas y Técnicas,
Universidad Nacional de Mar del Plata, Mar del Plata, Argentina

We analyze the behavior of blends containing a longitudinal polymer liquid crystal (PLC), namely PET/0.6PHB, where PET denotes poly(ethylene terephthalate), PHB is p-hydroxybenzoic acid, while 0.6 is the mole fraction of the latter in the copolymer. We consider the totality of results obtained experimentally, theoretically using statistical mechanics, and also by molecular dynamics computer simulations. Our PLC is oriented in magnetic fields that improve its mechanical properties and also can serve for reinforcement of engineering plastics. The resistance to deformation depends on the spatial distribution of the LC-rich islands phase in the LC-poor matrix.

Received 13 October 2001; in final form 25 October 2001.

A partial financial support of this work by the State of Texas and by the Robert A. Welch Foundation, Houston (grant B-1203) is acknowledged. Dr. Shreefal Mehta has participated in the magnetic field experiments. Mr. Ricardo Simoes has participated in the dynamic molecular simulations.

Address correspondence to Witold Brostow, Laboratory of Advanced Polymers and Optimized Materials, Department of Materials Science, University of North Texas, Denton, TX 76203-5310, USA. E-mail: brostow@unt.edu

Keywords: blends, channeling, critical-angle reflectometry, engineering polymers, LC island, magnetic fields, molecular dynamics, molecular models, PET/xPHB, phase diagrams, polybutylene terephtalate, polycarbonate, polyesters, polypropylene

1. INTRODUCTION

Two main directions of modern polymer technology exist: synthesis of new compounds and creation of new compositions by blending [1]. The latter one, which is becoming the most common route to produce new polymeric materials, entered the plastics industry half a century ago. At present, blends constitute by various estimates about half of the total plastics market. With progress in polymer science and engineering in the area of blending, one can expect further increase. The reason for the interest of industry in blends is the potential balance of properties not available in a single polymer. To succeed in blending, one should choose the components in accordance with certain fundamental rules.

One can begin with polymer pairs, completely *miscible* to give a homogeneous single phase. Such a blend will exhibit properties proportional to the ratio of the two polymers in the composition. However, a much larger number of polymer blends are created in which the constituting polymers are immiscible. Such a blend combining some of the best practical properties of each constituent might be quite useful. The term *compatible* is used for such systems [2].

A number of specific features may contribute to miscibility or lack of it: polarity, specific group attractions, molecular weight ratio and/or crystallinities of the components.

Polymers similar in structure or, more generally, similar in polarity are more likely to form miscible blends. Diverging polarities generally produce immiscibility. Polymers that are drawn to each other by hydrogen bonding, acid-base, charge- transfer, ion-dipole, donor-acceptor adducts, or transition metal complexes are less common, but when such attractions occur they are very likely to produce miscibility. Lower molecular weight permits a larger number of states on mixing and therefore a larger gain in entropy, which favors miscibility. Two polymers can be immiscible at approximately equal concentrations. However, at low concentration a minority polymer might be miscible in the main component. The properties of blends exhibit a strong dependence on their microstructures. When a single homogeneous phase is formed (miscible polymers), the properties are commonly proportional to the ratio of the polymers in the blend. For immiscible polymers, the phase rule takes its course. A system matrix + dispersed microdomains is created. A continuous matrix,

which controls most properties, is formed by a major phase; the minor phase will form dispersed microdomains and contribute to the properties to some extent. The key factor here is the structure of such domains, that is the material morphology. The nature of the interphase determines interactions between phases. The blended polymers should possess close melting or softening points so as to avoid premature degradation of one blend component.

Polyesters, widely used and considered an important class of polymers, can be manufactured as homo and/or copolymers [3]. Some copolymers contain in their main chains liquid crystalline groups, which impart liquid crystalline properties to the whole copolymer. Such materials—polymer liquid crystals (PLCs)–represent a rapidly expanding field of research due to their interesting behavior as well as advantageous properties. Engineering polymers (EPs) are typically flexible, with relatively low mechanical strength, low upper service temperature limit, and high thermal expansivity. By contrast, PLCs show clear superiority with regard to chemical resistance, low flammability and outstanding mechanical properties; the service temperature range is large; the isobaric expansivity is low, sometimes even values lower than zero are observed [4, 5].

With all these advantages, PLCs are more expensive than massively produced EPs. By blending the properties of PLCs can not only be manipulated but at the same time price can reach a reasonable level.

The fundamental mixing behavior of LC polyesters has been widely studied. They form miscible or partially miscible blends with a variety of polymers [6, 7].

In this paper we discuss the properties of polyester copolymers, from the principle "like to like" containing both phenyl and oxyethylene fragments. As a representative of this group copolymers of the type PET/xPHB of poly(ethylene terephtalate) (PET) and x p-hydroxy benzoic acid (PHB), where x denotes the molar fraction of PHB, will be discussed. This particular group also exhibits liquid crystalline properties. Such polymers were described many years ago by Kuhfuss and Jackson [8–11].

Blends of such copolymers, created according to the closeness of mechanical properties, shall be discussed. As representatives, we shall discuss in turn blends of polypropylene (PP), polybutylene terephtalate (PBT) and polycarbonate (PC) with PET/xPHB.

In the following, we shall consider in some detail the phase diagrams of polyester PLCs and their blends (Section 2). On this basis we shall be able to understand how to manipulate the phase structures as a key factor for processing and achieving desired properties of PLC blends with EPs (Section 3).

Then, in Section 4, we shall discuss how such blends can be represented as molecular models and how computer simulations help to understand the mechanical behavior of these materials. Section 5 deals with alteration of mechanical properties of polyester PLCs blends using strong magnetic fields.

2. PHASE DIAGRAMS

2.1 Introduction

Properties of materials, polymeric and otherwise, are of course determined by chemical composition as well as structure produced during processing. For PLCs, the situation is different than for engineering polymers because of the strong orientation acquired during processing and the influence of the high anisotropy on the mechanical properties (see Sections 3 and 5). While in some cases the anisotropy is desirable, controlling the resulting properties is possible only if we have enough knowledge of morphology and phase structures and also if we can locate each structure in the corresponding region of the phase diagram.

In 1988, Zachman and collaborators [12] have shown an example of a PLC phase diagram. In contrast to phase diagrams of non-LC polymer systems, their diagram shows a fairly large number of phase regions and a overall complexity. More specifically, the phase diagram of PET/xPHB—copolymers reported by us earlier—[13] has shown twelve different phase regions. In order to identify those phases and their transitions, a large number of techniques had to be used. The full diagram, including both non-equilibrium and equilibrium phases, is discussed below.

2.2 Phase Structures

Several investigations [14–17] suggested the existence of at least two phases: a LC PHB-rich phase and PET-rich phase. Scanning electron microscopy (SEM) results show the LC-rich phase as islands in the LC-poor matrix. This is important since understanding morphology is a priority to define processing conditions and influence final properties. This knowledge opens up new possibilities for polymer processing and in creating new types of materials. Thus, by cooling a PLC from nematic, smectic or cholesteric phases, it is possible to obtain films, glasses and coatings with the corresponding structures and achieve special properties unique to them.

The phase diagram of PET/xPHB copolymers as a function of x resulting from using a number of methods and also based on results of

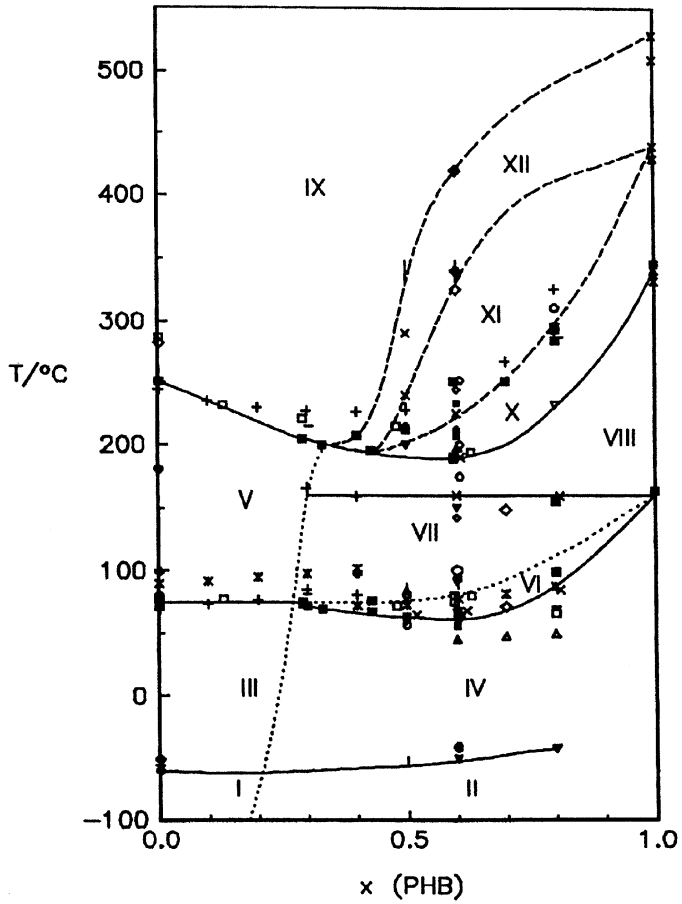

FIGURE 1 Equilibrium and non-equilibrium phase diagram of various PET/xPHB copolymers after [13].

different authors [13] is shown in Figure 1. *Non-equilibrium* phases, the corresponding transitions and the relaxational transition β *are* included.

The regions in the diagram marked with Roman numerals contain the following phases:

(I) PET crystals, isotropic glass (PET matrix with some PHB sequences), both below solid-state β relaxations.
(II) PET crystals, PHB-rich islands, isotropic PET-rich glass, PHB-rich glass, all below solid-state β relaxations.

(III) PET crystals, isotropic (PET-rich) glass, both above solid-state β relaxation transition.
(IV) PET crystals, PHB-rich islands, isotropic PET-rich glass, PHB-rich glass, all above solid-state β relaxations.
(V) PET crystals, quasi-liquid.
(VI) PET crystals, PHB-rich islands, PHB-rich glass, quasi-liquid.
(VII) PET crystals, PHB-rich islands, PHB-rich glass, quasi-liquid.
(VIII) PET crystals, PHB-rich islands, quasi-liquid.
(IX) Isotropic liquid.
(X) Smectic E, isotropic liquid.
(XI) Smectic E, smectic B, isotropic liquid.
(XII) smectic B, isotropic liquid.

Phase description includes the quasi-liquid (q-l) discovered in [13], which was in the amorphous state below its glass transition T_g but now is in the temperature range between T_g and the melting transition (which can be a transition into a mesophase). Except for elastomers, one calls such materials simply liquids. However, in the case of the PLCs, that name is not appropriate for several reasons:

(a) The quasi-liquid phase does not exhibit the ordinary liquid mobility. The presence of another component below its glass transition and/or of crystallites prevents the phase from flowing like a liquid does. This is in contrast to non LC polymers between T_g and T_m, where the formerly amorphous phase flows around the crystalline regions, with the liquid viscosity dependent for all purposes only on the temperature. The concentration of the quasi-liquid depends also on the concentration of LC sequences. In this context, we note the deuteron NMR results of Zachman and collaborators [12], who have found that in PET/xPHB copolymers the PHB sequences considerably decrease the mobility of PET sequences.
(b) The notion of a "liquid" brings about a mental association of a material which, upon heating, can only undergo vaporization or, if it is a polymer melt, no further transition at all. By contrast, the material containing a q-l phase has to undergo at least two more phase transitions: melting and isotropization at the clearing point. If more than one liquid-crystalline phase is formed, say smectic C and nematic, then there would be even more transitions.
(c) It is in the quasi-liquid phase that the process of so-called "cold crystallization" can occur.
(d) Finally, and as briefly noted above, q-l shows an analogy with the leathery state in elastomers. Both types of systems are immediately

above their glass transition regions, and both exhibit retarded reactions to application of external forces.

Inspection of Figure 1 shows higher degree of complexity because of the inclusion of β transition and non-equilibrium phases. Continuous lines correspond to localized transitions or relaxations. The nearly horizontal dotted line represents the maximum of cold crystallization, a process that also occurs at temperatures below and above the line. The nearly vertical dotted line represents creation of LC-rich islands, here also a region on both sides of the line is involved. The line is not quite vertical because as the statistical-mechanical theory of Flory and Matheson [18, 19], amplified in [20–22] shows, at lower temperatures an orientationally ordered (LC-rich) phase appears at lower concentrations.

The independence of the glass transition of the PET from x for low x values indicates that the solubility of PHB in the PET-rich phase is quite low, while the PHB-rich phase allows relatively higher concentrations of PET. The further increasing in PHB content up to $x = 0.6$ decreases the glass transition of the PET. This suggests the presence of a non-random chain structure–resulting in regions that are richer in PET or in PHB. If the system were random, one would expect and increase in T_g of the PET due to the addition of the stiff PHB units along the backbone.

There is a depression of the melting point T_m from 251°C for pure PET to 212°C for $x = 0.6$ PHB. The values of T_m indicate that the melting is due to PET regions, with incorporation of PHB segments causing dilution effects.

An intelligent approach to define processing conditions knowing the phase diagram has been proposed. Assuming that during processing both components should be completely melted and the anisotropic polymer should exhibit liquid crystallinity, the processing temperature range can be now defined using the phase diagram we have just considered.

3. POLYESTER AND PLC BLENDS

As already noted above in comparison to engineering thermoplastics, PLCs show superior mechanical properties, chemical and fire resistance among other properties. Mainly because of PLCs prices, blending with flexible thermoplastics is an attractive method for creating new materials at an affordable cost.

During the last 20 years rheology, morphology, and mechanical properties of PLCs and thermoplastic blends, including polycarbonate (PC), polystyrene (PS), polyethylene terephthalate and polyamides (such as nylon 6/6) among others, have been studied. We note that the process of forming an elongated thermotropic PLC fibrous structure in-situ depends on factors such as the relative composition, the interfacial tension, the viscosity ratio, and the flow field involved in the processing procedure [23]. We have studied blends of the longitudinal thermotropic PLC PET/0.6PHB with PC, PP, PET and polybutylene terephtalate (PBT) [13, 14, 17, 24, 25].

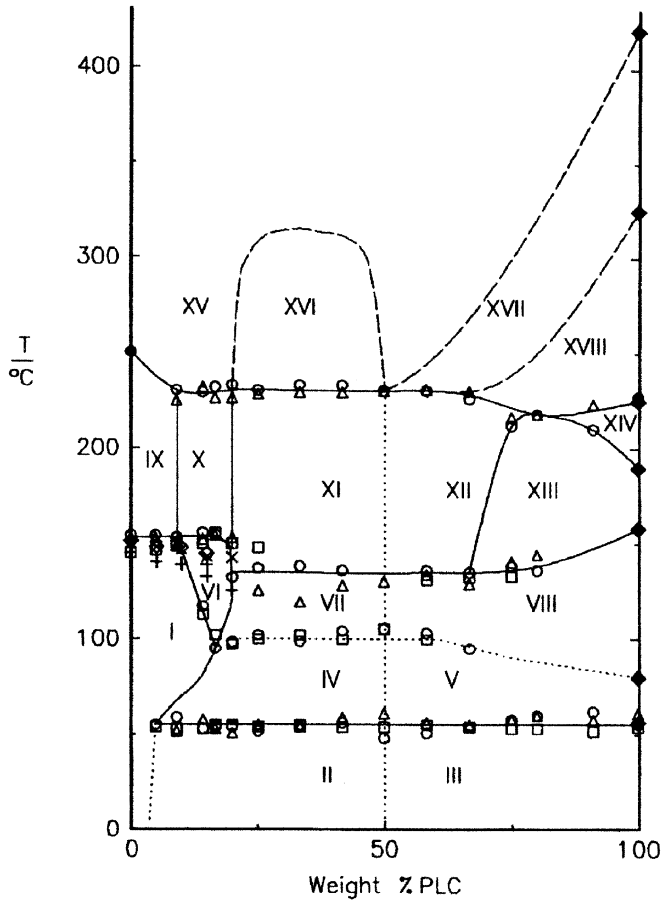

FIGURE 2 Phase diagram of PET/0.6PHB + PC system, results for samples precipitated from solution and annealed 60 min.: △ DSC □ DMTA ○ TMA; for injection molded samples without annealing: ◇ DSC × DMTA + TMA; after [26].

TABLE 1 Description of Regions Found in the Phase Diagram for PET/0.6PHB + PC

Phase	States	
I	PC rich glass	PC crystals
II	PC glass	PC crystals PET glass
III	(PC + PHB) glass	PHB-rich islands PET glass
IV	Glass	PC crystals quasi-liquid
	PET crystals (small amounts)	
V and VIII	Glass	PET crystals quasi-liquid
	PHB Islands	
VI	Glass	PC crystals quasi-liquid
VII	Glass	PC crystals quasi-liquid
	PET crystals	
IX	PC crystals	i-liquid
X	quasi-liquid	PC crystals i-liquid
XI	quasi-liquid	PC crystals i-liquid
	PET crystals	
XII	quasi-liquid PET crystals	PC crystals PHB-rich islands
XIII	quasi-liquid	PET crystals PHB-rich islands
XIV	Smectic E	i-liquid
XV	i-liquid	
XVI	(PC + PET) rich liquid	PHB rich liquid
XVII	i-liquid	Smectic B
XVIII	i-liquid	Smectic E Smectic B

3.1 PLC PET/0.6 PHB and PC Blends

The phase diagram of PLC and PC blends resulting from the use of DSC, TMA and DMTA is presented in Figure 2 [26]. Table 1 contains the description of the regions presented in the diagram. The phase diagram shows a T_g at 62°C, which is due to PET phase present in PLC. This transition is found by DMTA, TMA and DSC; it is independent of the blend composition and is the same as that of the pure PET. On the other hand, the amorphous PC shows a T_g at about 150°C. This transition is greatly affected, not only by the thermal history but also by the mode of preparation of the samples. Annealing at 210°C produces no effect on 62°C transition. However, increasing the annealing time from 1 to 60 minutes produces 50 K decrease of T_g of the PC. This behavior is explained by a gradual increase of the miscibility during annealing. The concentration of the PLC in the PC phase increases; therefore, the T_g of the PC decreases. The area between the PET T_g and the PC T_g includes the quasi-liquid (q-l) phase defined in Section 2.2.

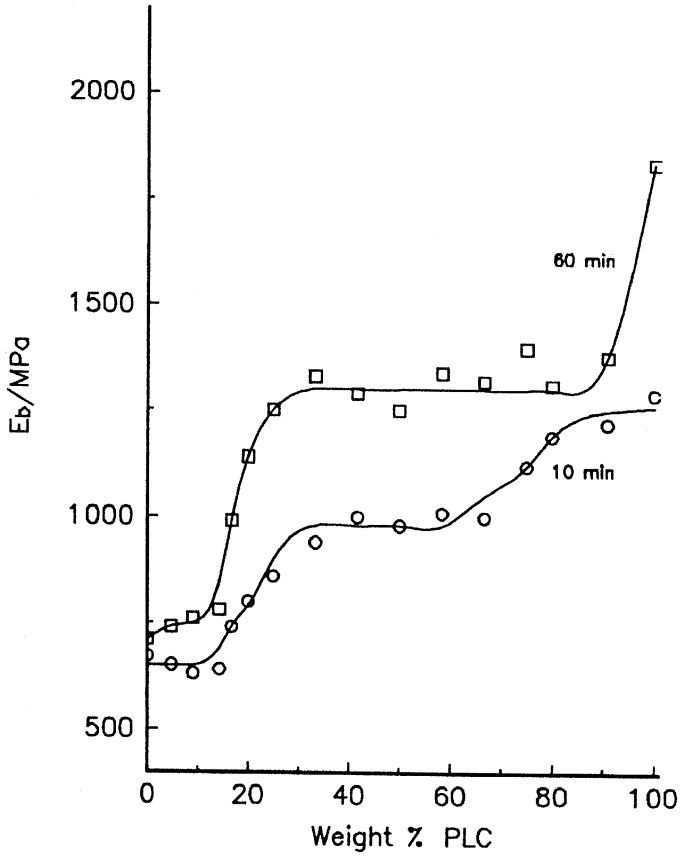

FIGURE 3 Flexural modulus of PC + y% PLC system as function of concentration, indicated time of annealing; after [26].

3.1.1 Mechanical properties

The interaction between PLC and PC has important consequences for the mechanical properties. Figure 3 shows the influence of annealing time on the flexural modulus as a function of the PLC concentration [26]. It is clear that longer annealing times between 210°C and 220°C increase the modulus because of the increased crystallinity discussed previously. Results of tensile properties (Figures 4 and 5) also show the reinforcement effect of the PLC [26]. Samples were extrusion blended and injection molded. For low deformations there is a reinforcement effect due to the rigidity of PLC. Therefore, the elastic modulus increases not only in the direction parallel to the flow but also in the perpendicular one. At higher deformations

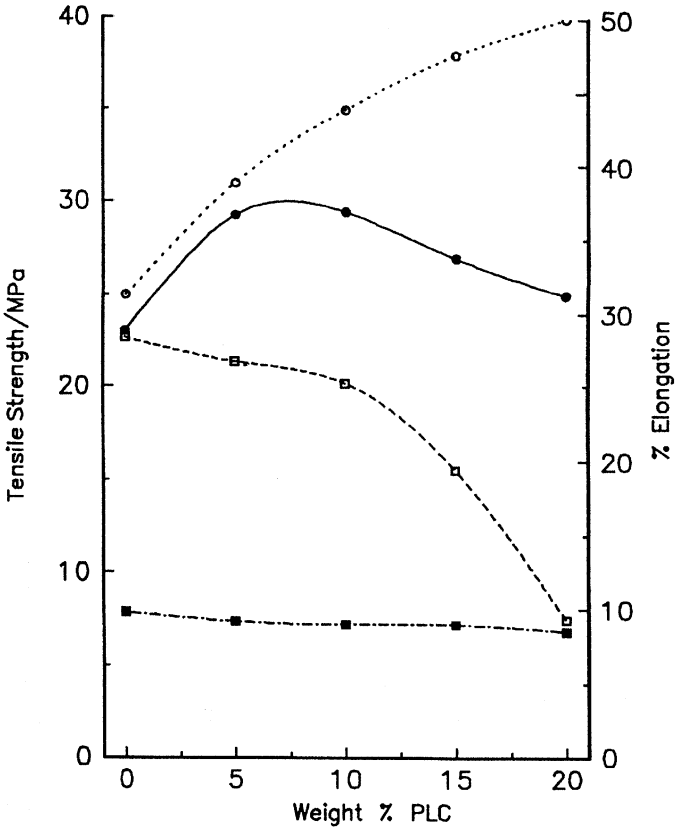

FIGURE 4 Tensile strength σ and % elongation as function of composition of PC + PLC: ○ σ parallel, ● σ perpendicular, □ % elongation parallel, ■ % elongation perpendicular; after [26].

orientation of the samples and interfacial adhesion between PLC and PC become more important. Thus, the yield strength and the tensile strength measured in directions parallel to the flow increase with PLC content. On the other hand, the same properties measured in the direction perpendicular to the flow slightly increase up to 10% PLC, the composition where good miscibility in the glassy state is observed, but then decrease for higher concentrations of the PLC. The elongations at break are lower for samples oriented perpendicularly to the flow than for the parallel samples. The tie-molecule regions of the PC play a dominant role in determining the elongation since the rigid sequences do not expand significantly.

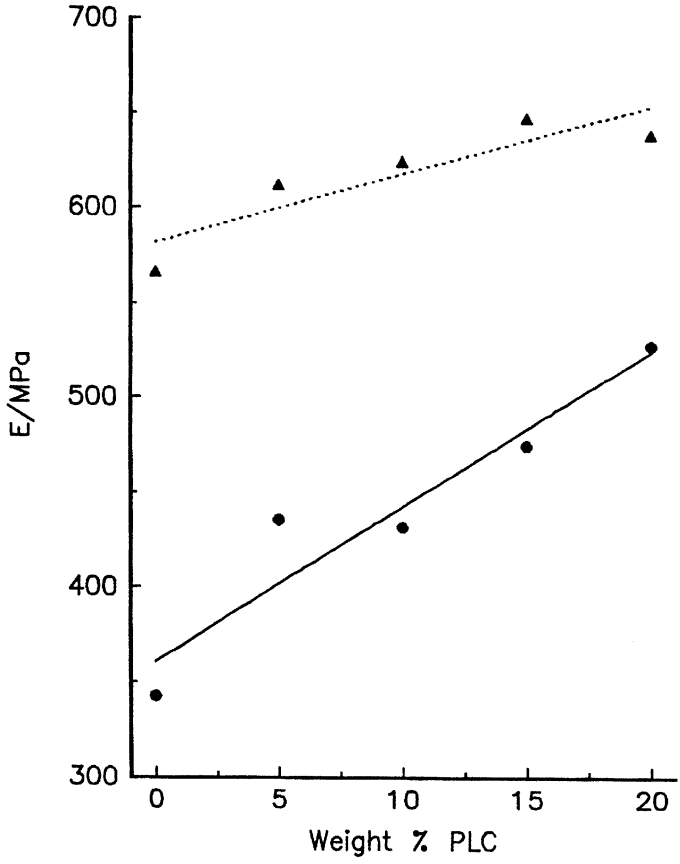

FIGURE 5 Elastic modulus as a function of composition of PC + y% PLC in ○ perpendicular and △ parallel direction to the flow; after [26].

3.2 PLC PET/0.6 PHB + PBT Blends

The partial phase diagram of blends containing up to 20% PLC based on the DSC and DMTA data is shown in Figure 6 [27], which also includes the β transition of PBT. The different regions showed in the diagram are described in Table 2 [27]. Along with the β transition of PBT and increasing the temperature, the diagram shows T_g of PBT, T_g of PET, crystallization and melting of PBT.

Again, an important advantage of having the phase diagram is to determine the processing temperature range and composition to be selected in order to develop melt-processable liquid crystal and flexible polymer blends. Because of the anisotropy desirable in the

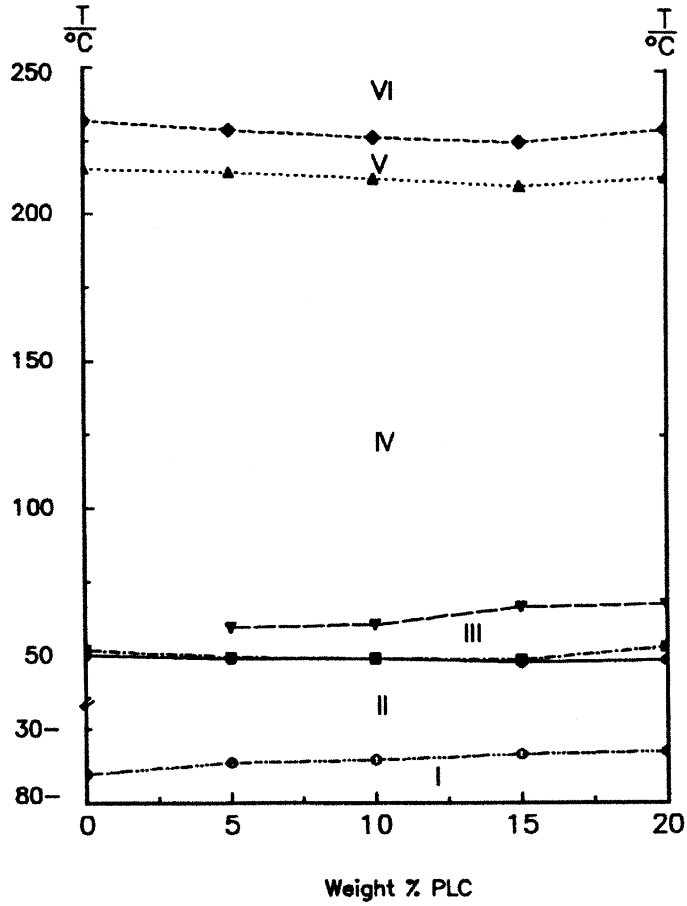

FIGURE 6 Phase diagram of the PET/0.6PHB + PBT system; △ T_c PBT ▼ T_g PET ■ T_g PBT (DSC) ◆ T_m PBT ○ T_β PBT ● T_g PBT (DMTA); after [26].

dispersed phase –PLC– in order to get alignment in the flow direction, the blend should be process in conditions corresponding to region V.

3.2.1 Mechanical properties

Elastic modulus E, tensile strength and elongation at yield point, and strength and elongation at break for blends of PBT and PLC are shown in Table 3 [27]. The results indicate that both the Young modulus E, the tensile strength at yield point σ_y and the break

TABLE 2 Description of Regions Found in the Phase Diagram for PBT + PET/0.6PHB

Phase	States	
I	PBT glass	PBT crystalline
	PET glass	PHB islands
II	PBT glass	PBT crystalline
	PET glass	PHB islands
III	PBT crystalline	PHB islands
	PET glass	
IV	Quasi-liquid	PBT crystalline
	PET crystalline	PHB islands
V	Quasi-liquid	PBT crystalline
	Smectic E	PET crystalline
VI	Isotropic liquid	Smectic E
	Smectic B	

strength σ_u increase with increasing PLC concentration. The influence of the orientation is evident since the tensile strength and the modulus in samples oriented perpendicularly are smaller than those for samples oriented parallel to the flow. The increase in stiffness can also be related to orientation and fiber formation of the PLC matrix. An island structure characterizes the blend oriented perpendicularly, while a fiber-like structure is present in the blends oriented parallel to the flow. Elongation at yield El_y and elongation at break El_u decrease with increasing amount of the PLC and are dependent on the PLC-induced anisotropy. Both elongations are consistently higher along the direction parallel to the flow than

TABLE 3 Mechanical Properties of PBT + PET/0.6PHB Blends

% PLC	Sample Orientation	σ_y MPa	% El_y	E MPa	σ_u MPa	% El_u
0	Per.	11.7	5.15	634	10.6	4.2
5	Per.	15.2	1.40	681	12.1	3.9
10	Per.	17.2	0.85	689	13.0	1.4
15	Per.	18.1	0.85	743	13.3	1.0
20	Per.	19.7	0.85	754	14.2	0.9
0	Par.	12.4	5.2	672	11.7	7.2
5	Par.	27.4	5.1	1735	22.3	7.1
10	Par.	29.2	3.6	2165	24.1	5.4
15	Par.	30.1	3.1	2438	25.3	4.7
20	Par.	30.4	3.1	2769	25.9	3.8

perpendicular. In summary, the PLC addition to PBT has made the engineering polymer stiffer but more brittle, particularly in the perpendicular direction.

3.3 PLC PET/0.6 PHB + PP Blends

As was pointed out in the previous section, transitions need to be evaluated by different techniques. In PP and up to 20% PLC blends the only transition clearly observed by DSC is the melting point of PP. The T_g of the PET in the PLC phase cannot be detected since its concentration is low and its corresponding thermal effect low. The partial phase diagram of PP + PLC blends showed in Figure 7 was built from data obtained from DSC and DMTA runs [27]. The phases involved are described in Table 4.

3.3.1 Mechanical properties

As was pointed out before, mechanical behavior is influenced not only by PLC orientation (see Section 5) but also by interfacial adhesion between the composite components (see Section 3.3). The tensile strength behavior of blends PLC + PP show both influences. Up to 10 PLC%, both σ_y and σ_u slightly increase—about 5%—in samples oriented parallel to the flow, see Table 5. Further PLC addition decreases both σ_y and σ_u. Poor dispersion and/or lack of adhesion are responsible for the maxima. Morphology studies indicate that the adhesion between the two phases is better at low concentrations [27]. On the other hand, elastic modulus is substantially enhanced over that of pure PP when increasing PLC content up to 10%, and then remains practically constant. The increase in modulae can be attributed to the presence of the reinforcing LC sequences in the chains.

3.4 Rheology of Polyester + PLC Blends

It has been found that addition of PLC to polyester results in blends with lower viscosity [28]. In certain instances the viscosity of the blends was two to three times lower than that of the respective polyester matrix. Thus, modification by PLC results in a considerable increase of the processability of the matrix studied. Significant effects appear at PLC concentrations as low as 5 wt%.

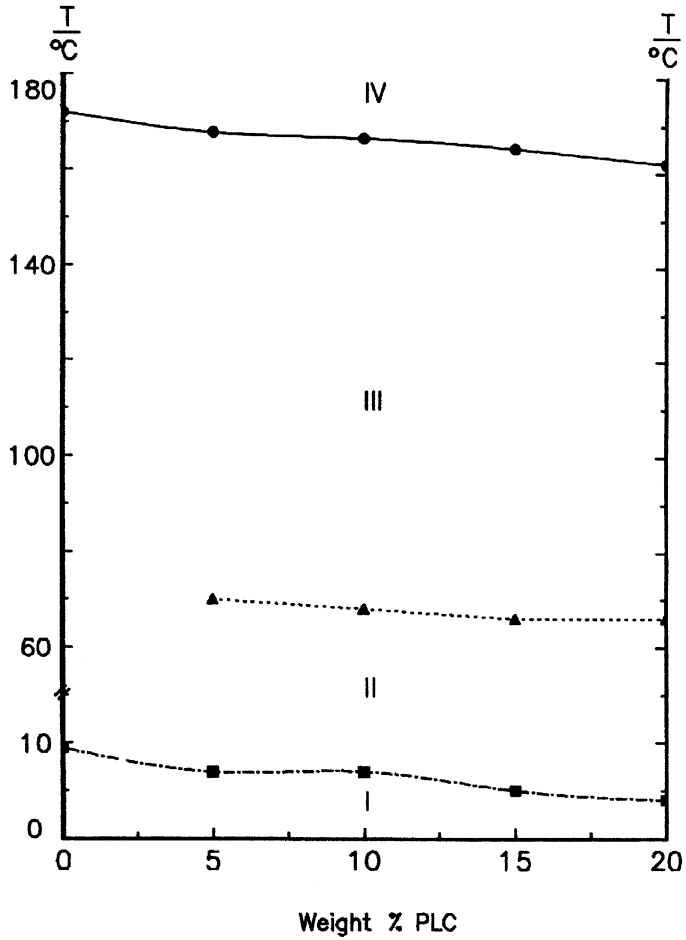

FIGURE 7 Phase diagram of PP + PET/0.6PHB system; ▲ T_g of PET ■ T_g of PP ● T_m of PP [26].

3.5 Reactive Compatibilization

The results of many studies of polyester PLCs blended with thermoplastic polymers suggest the need for achieving better interfacial adhesion. The adhesion between phases of a PLC + thermoplastic blend is often poor because of the intrinsic incompatibility of the two materials. The lack of adhesion between phases greatly reduces the transverse and shear strengths of the blend. Interphasic interaction depends on the specific chemical structure of the macromolecules of

TABLE 4 Description of Regions Found in the Phase Diagram for PP + PET/0.6PHB

Phase	States	
I	PP glass	PP crystalline
	PET glass	PHB islands
II	PBT glass	
	PP crystalline	PHB islands
III	Quasi-liquid	PET crystalline
		PHB islands
IV	Isotropic liquid	PHB islands

both polymers in the blend. From the already mentioned principle of "like to like," it is desirable to utilize compatibilizers, i.e. block copolymers with segments capable of specific interactions and/or chemical reactions with PLC or both constituents. It has been also reported that graft copolymers act as polymeric surfactants reducing the interfacial tension, which promotes interphasial adhesion [29].

J.F. Croteau et al. [30] show that the adhesion between poly (hexamethylene terephtalate) (PHMT) and PET/xPHB increases because of the reaction in the melt. Laivins [31] concludes that a transesterification reaction occurs during the melt blending between PET/0.6 PHB and PHMT. Blends of PP and polyester PLCs have been compatibilized by adding maleic anhydride-grafted-polypropylene (MAGPP) [32]. Larger improvement has been obtained using MAGPP with PP and polyester-co-amide PLCs. These results suggest that the final properties of blends are not only determined by the amount and

TABLE 5 Mechanical Properties of PP + PET/0.6PHB Blends

% PLC	Sample Orientation	σ_y MPa	% El_y	E MPa	σ_u MPa	% El_u
0	Per.	14.9	8.7	367.2	10.1	13.1
5	Per.	14.3	6.0	449.2	8.6	7.7
10	Per.	12.9	4.7	449.0	8.4	4.7
15	Per.	10.7	4.0	448.7	6.3	4.5
20	Per.	9.4	2.4	449.7	4.9	3.3
0	Par.	14.9	10.6	368.3	10.1	28.8
5	Par.	15.4	7.8	413.0	10.2	13.8
10	Par.	15.6	6.7	457.2	10.7	10.0
15	Par.	12.5	4.7	464.9	9.4	5.3
20	Par.	12.0	4.1	469.0	8.3	4.6

properties of the reinforcing PLC but also by the efectiveness of the compatibilizer [33].

4. MOLECULAR MODELING OF PLCs

4.1 Reasons for Performing Computer Simulations

The development of computer technology has provided the tools that make possible—at least in principle—a comprehensive understanding of a variety of physical systems that have previously been very difficult to study. Especially in the area of fracture and deformation, computer simulations can provide step-by-step analysis of material failure. This is a way of creating complex structures and investigating them at the molecular level, a level that is hardly accessible to laboratory experimentation.

Given a fair experiment-based description of PLC systems, one can decide which known features are the most important and primarily influence their behavior. This is the first step needed to produce a mathematical model, the beginning of the computer simulation. If the model is simple, predictions will be easy to make but could be wrong. If the model is too complex, the predictions might be more realistic but they might be hard to make in the first place. Even if one tries to walk the middle ground, it often happens that the model via a theory leads to conclusions that do not agree with the experiment. The probable reason for the disagreement, except for experimental or mathematical errors, is that at least one important feature of the system was not included in the model.

The missing feature or features can be best found by doing computer simulations. The model implemented on the computer is exactly that assumed for the system. Hidden variables that lurk in nature are eliminated. If there is a disagreement, now it cannot be blamed on experimental inaccuracies. If there are problems in the mathematical approximations made in deriving the predictive equations, they will become visible [34].

The theory and the "computer experiments" are both based on exactly the same model. Parameters of the model can be varied to see how simulation results depend on them. Assumptions of the computer model can be varied as well to see which were realistic and lead to sensible results and which were, in fact, the root(s) of the problem(s). Improved understanding of the system and a better model with enhanced (or possibly even correct) predictive capabilities is a typical result. After verification and validation of simulations, the model is ready to work [35].

4.2 Simulation Procedures

Among computer simulations, which have been applied in polymer science and engineering, three basic types can be distinguished, namely molecular dynamics (MD), Monte Carlo (MC), and Brownian dynamics (BD). The last of these is mostly applied to polymer solutions [36,37] and will not be discussed here further.

The MC method has an interesting history. In the late 1930s, a group of Polish mathematicians associated with the King John Casimir University, now Ivan Franko University in Lviv, and which included Stanislaw Ulam, spent much time in the Scottish Cafe near the university. Somebody in this group suggested that winning in roulette (taking the bank) in the casino in Monte Carlo is really a problem in mathematics. Interesting attempts to solve the problem were advanced and argued about, until World War II broke out in 1939. The original problem was never solved, which is why the casino in Monaco is still in business. However, when Ulam emigrated to the United States, he found some of the results obtained in the Scottish Cafe useful for other purposes. Because of the war and the dispersion of the original participants around the globe, Metropolis and Ulam published the Monte Carlo procedure only in 1949 [38].

MC relies on making one step at a time and taking stock of the situation after a certain number of such steps. Applying MC to material systems, we create an object that consists of N particles such as polymer segments (or atoms, or monoatomic molecules or ions). One can construct a 6N-dimensional phase space since each particle has three coordinates of position (for instance the Cartesian ones) plus three coordinates of momentum. One calculates the equilibrium properties of a system by averaging over a large number of states of the system, each state created by the MC procedure. For instance, one can determine experimentally the average radius of gyration $\langle R_g \rangle$ of a polymer. MC gives us two ways of obtaining $\langle R_g \rangle$. One can either obtain a large number of chains and perform averaging over them. Or, one can create just one chain, perform 20000 MC steps and average over all these states of a single chain. Statistical mechanics tells us that the resulting $\langle R_g \rangle$ should be the same. Because of its nature, MC is well suited for the evaluation of equilibrium properties.

MD was first developed by Berni J. Alder and collaborators in 1957 [39]. Again consider a system of particles, each at a given time at a location specified and with velocity (or momentum) also specified. In contrast to MC, in which one particle moves at a time, here we let all particles "run" at once. The velocity $v_i(t)$ of the ith particle at time t can be for instance calculated as:

$$v_i(t + \Delta t/2) = v_i(t - \Delta t/2) + F_i(t)\Delta t/m_i \quad (1)$$

Here Δt is the time step assumed for the simulation, $F_i(t)$ the force acting on the ith particle, and m_i the mass of the particle. $F_i(t)$ is calculated from potentials that describe interaction between particles (more on this subject below). Since MD time is an explicit variable, the method can be used to simulate not only equilibrium properties but also time–dependent ones. This is particularly important for viscoelastic materials with which we are dealing; MD gives the capability to investigate processes such as diffusion flow and fracture. This is a powerful feature, since the motions of polymer chains constitute the key to understanding their properties.

4.3 Creation of Material on a Computer

PLCs are relatively complicated; systems of flexible macromolecular chains are simpler. A task simpler still consists of creating a *metallic* material, that is a system of molecules which are monoatomic. A convenient structure on which one can place the atoms is the two-dimensional hexagonal lattice. The lattice has several advantages: all nearest neighbors are equivalent (compare the square or the simple cubic lattice); the coordination number is $z = 6$, a value which occurs typically in real three-dimensional lattices; at the same time one retains the perspicuity resulting from the two-dimensionality of the lattice. Thus one can start with a metallike lattice first (chains of one particle each) and then include the connectedness between the particles.

There are several methods of creating polymer chains and a good one was developed by Mom [40]. The essential step consists of finding two chains such that an end particle of one of them is a nearest neighbor of an end particle of the other chain. When such chains are found, they become connected, forming one longer chain. Thus, the total number of chains in the material decreases by one. Needless to say, the process is quite easy at the beginning, then more and more difficult, and at some point no more chains can be connected in this way. In the Mom procedure the system is then scanned to see whether there is a particle inside one of the chains that is a nearest neighbor of one of the end particles of another chain. When such a particle is found, a part of the former chain is connected to the latter. In such a way the number of chains does not decrease, but the lengths of both chains change while new particles appear on their ends. A random choice is made to accept or reject such a move, this to prevent an infinite loop into which the program execution might fall. The Mom

method fails when in all chains the end particles are surrounded by particles belonging to the same chain. For such a case, Blonski, one of us and Kubat developed a modification of the Mom procedure [41]. A particle is sought that is the nearest neighbor of an end particle of the same chain. Then the chain is rearranged so that the particle becomes connected to the old chain end and it becomes the new chain end. Such computer generation procedures are relatively time consuming (in one case 18,532 iterations were needed to create a system with 3600 particles). However, polymeric materials with realistic features are created as confirmed also by MD simulations of stress relaxation [41].

Once a flexible polymeric material is generated, making some sequences in all chains rigid so as to achieve a prescribed concentration θ of LC sequences in the material may generate a PLC. There is a potential of interactions u(R) (where R is the interparticle distance) between flexible segments inside a chain. The rigidity is achieved by introducing a different potential [42]; see Figure 8.

The double well for the flexible + flexible interactions mimics the *cis* and *trans* conformations in carbon–like chains. At large intersegmental distances bond scission is possible—an important feature when studying behavior in mechanical force fields.

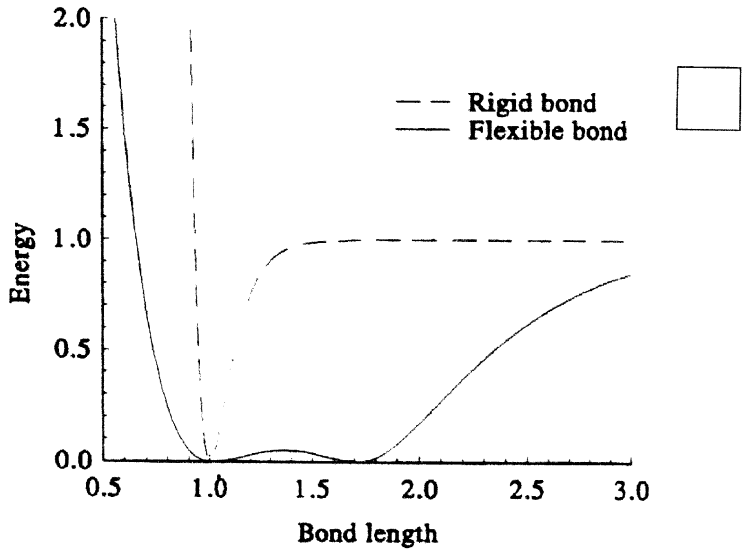

FIGURE 8 Binary interaction potentials used in the simulations. The flexible potential incorporates a double well, making possible conformational transitions, (such as *cis* to *trans*); after [34].

It has been found experimentally that above a certain critical concentration $\theta_{\mathrm{LC\ limit}}$ the LC sequences form a separate phase [13, 14, 43, 44, 45]. That phase constitutes islands in the flexible matrix. The next problem is thus creating islands on the computer of appropriate shapes and sizes. Here once again computer simulations have an advantage over experiments. Experimentally one cannot create islands of the desired size or shape; on the computer it can be done easily, and shapes such as ovals, diamonds or squares have been created [46].

The rigid LC island configurations created correspond to the three–dimensional island configuration as closely as possible: circles and ovals are the two–dimensional equivalents of spheres and ellipsoids.

In polygonal configurations, especially with relatively large dimensions, geometry within the lattice is far from uniform. This poses the problem of obtaining an accurate concentration measurement while maintaining relatively uniform distances between neighboring islands. Of course, with purely rectangular island configuration, a small portion of lattice could be created and then simply repeated to produce a larger representation. Due to the irregularity of the polygonal island this could not be done. Brostow et al have been developing procedures capable of creating computer-

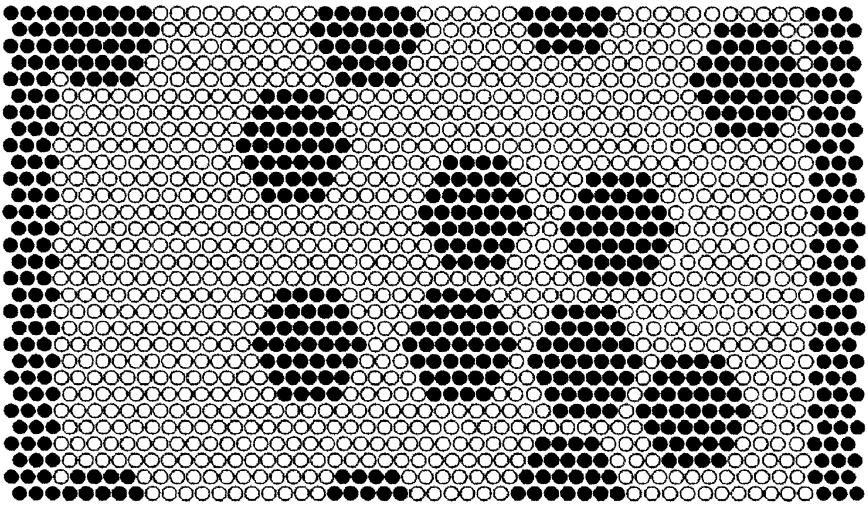

FIGURE 9 A computer–generated PLC. LC islands are represented by dark polygons. Dark dots represent rigid elements, light ones – flexible parts; after [45].

generated PLC with random LC island positions at different LC concentrations [47].

The simulation of PLCs can be well performed using the constant temperature MD procedure as described, for instance, by van Gunsteren [48]. As seen in Equation 1, the Newton differential equations of motion are transformed into difference equations employing the finite time step Δt. One also sees that the velocities at the time $t + \Delta t/2$ are calculated from those at the time Δt earlier. One usually works for simplicity with reduced (dimensionless) values of energy, distance, time, temperature and mass [49].

To calculate the forces, one has to know which particles (in PLC simulations these are segments, i.e. flexible or rigid) constitute neighbors of a given particle; otherwise the calculation would be longer than necessary while the results are the same. Efficiency in the simulation can be achieved by renewing the list of pairs of nearest neighbors after each time step [40]. Thus, dynamic changes in the system are recorded until the end of the simulation—usually defined by the fracture of the material.

It is important to maintain the temperature constant. This can be achieved by multiplying the velocities of the particles at every time step by a factor λ defined as

$$\lambda = \{1 + 0.05(E_{k0}/E_k - 1)\}^{1/2} \tag{2}$$

where E_{k0} is a predefined value of the kinetic energy of the systems while E_k is the actual value of that energy. E_{k0} is of course defined in terms of the temperature to be maintained: the multiplying factor 0.05 assures that the coupling is sufficiently weak.

The periodic boundary conditions are used to eliminate possible problems resulting from the finite size of the system. This is because one cannot create one mole of particles on a computer; even if one could, the time of a single run would be too long. If the system is contained in a cubic box then 26 identical copies ("ghosts") are built on the computer around it. Whenever a segment makes a move such that it leaves the central box, a "ghost" of that segment automatically enters the box from the opposite side. Thus the number of segments in the box remains constant and we do not have to worry about surface effects. This is important for systems consisting of a finite number of chains of finite length. The equivalence of averaging over systems with averaging over time for a single system has been mention earlier. The equivalence applies to an infinite number of systems on one side and an infinite time on the other. In practice, one generally tries

to build a system as large as possible consistent with getting results within a reasonable time.

4.4 Response of PLC to Tensile Stress Seen in MD

Development of a MD code, which would create systems of PLC chains on the computer and then subject them to external mechanical forces, is apparently not quite easy in spite of the principles defined above.

As mentioned above, the problem of *validation* of the simulations is important too. Therefore the first and obvious question is: does the system created on a computer as described above and with interaction potentials shown in Figure 8 really behave as a real polymer? We shall discuss this in the next subsection.

To answer this question, let us take a closer look at a tensile "experiment" with the computer generated material. A simulation of its stress - strain behavior has been performed [42,47]. The results are shown in Figure 10 for different LC segments concentration. One can see that the computer-generated diagram of stress vs. strain has all the features of such diagrams known from experiments.

Once again, the PLC sequences in chains provide reinforcement together with an increment of brittleness. The computer simulations

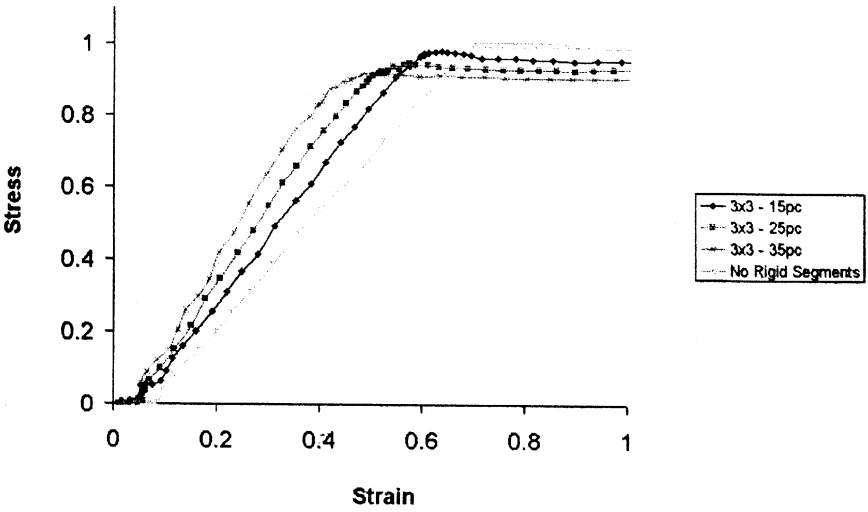

FIGURE 10 Stress–strain curves, generated in MD simulation at different PLC concentration. The assumption was made that all islands are of the same size, after [46].

confirm this fact. Thus the validation of the simulated system has been accomplished.

4.5 Cracking

An interesting aspect of mechanical behavior one can simulate using the model described above is *cracking*. When in neighboring and locally aligned chains there is a bond scission along a line perpendicular to the alignment, a crack is formed. However, since in carbon–like chains *cis* and trans conformations are allowed (see again the double – well interaction potential in Figure 8), the first effect of the application of tensile force is the *cis* → *trans*conversion.

The starting point is presented in Figure 11 (a) for the undeformed material with random arrangement of PLC islands. At the beginning of the simulation (b) the cis → trans conversion occurs on the right hand side. With increasing stress, the conversion appears also on the lefthand side (c). Next the remaining part of the material in the middle is converted (d). When all *cis* → *trans* conversions have taken place, the chain relaxation capability (CRC) [50] has been exhausted. Further introduction of energy into the system during deformation leads to crack formation (e) and then crack propagation; the crack has propagated approximately along the LC island line (f).

The next example we consider is molecular modeling of crack propagation in an oriented material. LC islands are here distributed equally along horizontal and perpendicular directions. The first such example is a computer-created material with LC islands net having a square as a basic unit. Now one can observe the mechanism of crack initiation and crack propagation inside the aligned material. Behavior here is somehow similar.

The starting point is presented in Figure 12 (a), (b) and is analogous to that pictured in Figure 11. Then, the conversion appears in the mass of material between lines, where initial conversion occurs, on the lefthand side (c). Next the remaining part of the material in the middle is converted (d). Further, cracks appear (e) in organized manner. Then cracks propagate and connect, causing fracture of material (f).

Another structure that can be considered consists of LC islands on a lattice with the hexagonal basic unit.

Again Figure 13 (a) and (b) are somewhat similar to Figures 11 (a), (b) and 12 (a), (b). Then with driving stress the conversion appears along every single line of islands and the remaining part of the material is converted in wave-like manner(c). In Figure 13 (d), crack is

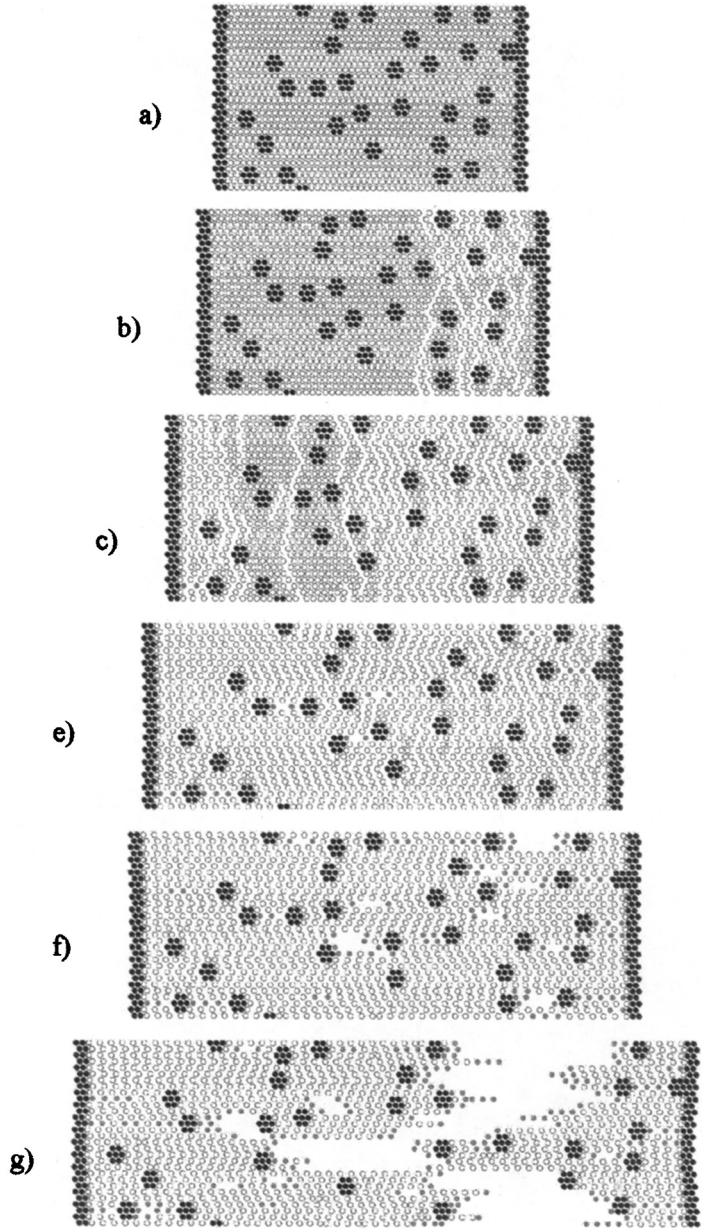

FIGURE 11 MD simulation of crack propagation in PLCs, after [46].

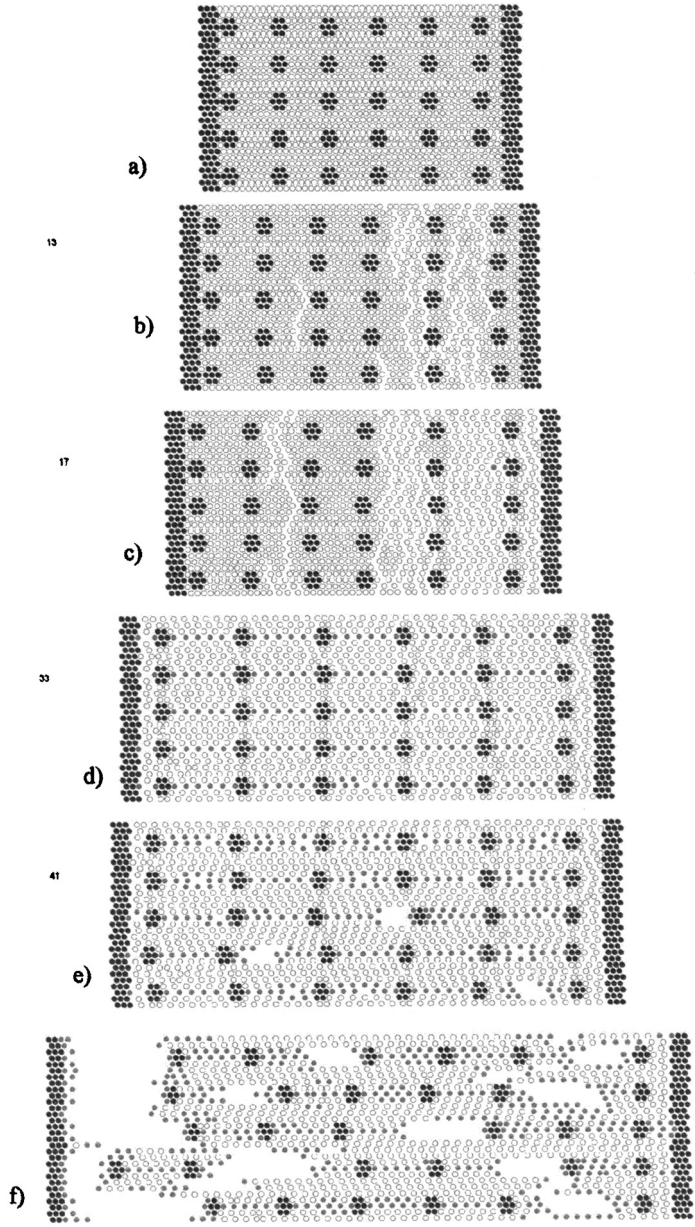

FIGURE 12 MD simulation of crack propagation in aligned PLCs, after [46].

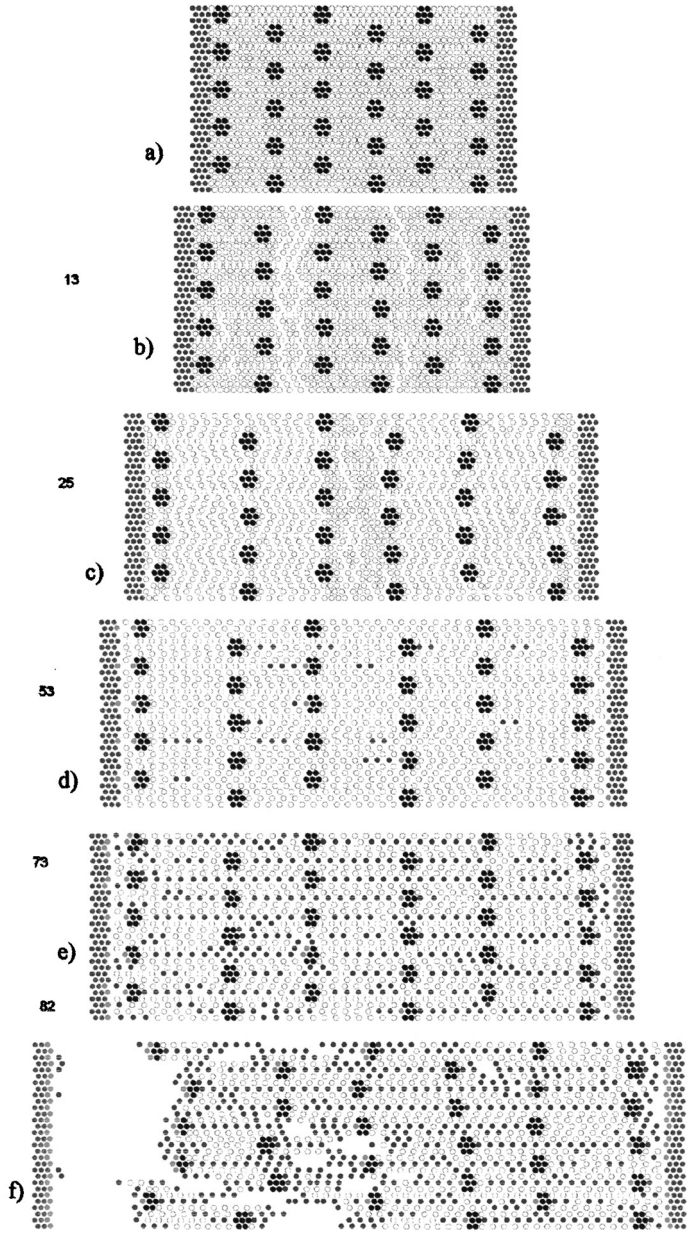

FIGURE 13 MD simulation of crack propagation in aligned PLCs, after [46].

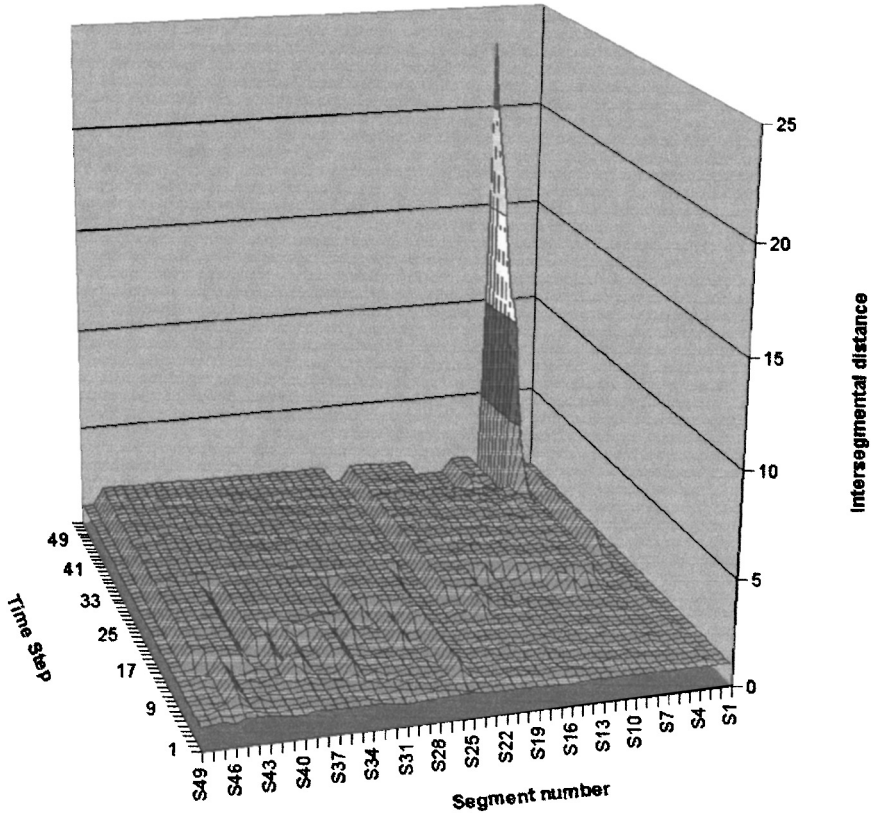

FIGURE 14 Time–distance dependence for one chain only, after [46].

formed. This process progresses (e) and then crack propagation leads to final fracture (f).

As presented above, MD simulations of PLC material enable to study also the intermediate cracking stages: from the conformational conversions via crack formation to the crack propagation shown in Figures 11–13.

Studies of changes in the intersegmental distance with time and stress can be performed as well. In Figure 14 we can observe this change in one chain, a particle after particle up to the moment, where distance increases rapidly which results in a bond scission. Note the rigid particles do not change distance and the deformation of the chain is carried by flexible particles.

A tacit assumption was made above, namely that the simulated PLCs were all longitudinal. We recall that there exist also other

classes of structure of PLCs, as discussed in [4] and [5]. In the future, MD simulations should be able to elucidate mechanical behavior of other classes of PLCs synthesized by chemists.

5. BEHAVIOR OF LIQUID CRYSTALLINE PET/XPHB BLENDS IN MAGNETIC FIELDS

Central to liquid crystalline properties is the anisotropy of shapes and interactions of molecules or their parts [18–22]. Once exposed to a magnetic field, the molecule possesses an induced magnetic dipole; the dipole will tend to orient with its north and south poles along the magnetic field. Induced magnetic dipoles, parallel as well as perpendicular to the long axis of the molecule, are possible. Therefore, LC molecules tend to align in either parallel or perpendicular fashion with respect to the magnetic field. The presence of the field causes a LC sample to acquire a magnetic dipole. The magnetic dipole per unit volume of the LC is defined as its magnetization [51]. We know that in LCs, that is both in monomer liquid crystals (MLCs) and in PLCs, the MLC molecules or their rigid LC sequences in PLCs are oriented approximately parallel to a preferred axis in space called *director* [52]. A magnetic field applied parallel to the director, while the director is locked in its position, induces a certain amount of magnetization; necessarily a magnetic field applied perpendicularly to the director induces a different amount of magnetization. Since the director can easily change its orientation, PLCs can interact with external magnetic or electric fields. Such interactions manifest themselves as changes in material structure caused by changes in the alignment.

The ratio of the magnetization to the strength of applied magnetic field is usually constant and is called the magnetic susceptibility. PLCs have two magnetic susceptibilities: one for fields applied perpendicularly to the director and one for parallel fields. Both necessarily vary with the temperature [51].

The effects of external magnetic field imposition on PLCs can be divided into two phenomena:

1. changes in the microscopic structure of the mesophase; the field stabilizes the distribution of the directors, no macroscopic changes occurs;
2. due to destabilization and reorientation of the directors, changes in macroscopic structure occur; such a transition from an undeformed to a deformed texture is called the Freedericksz transition; this is *not* a phase transition, because at any point in the liquid

state the order of the molecules relative to one another remains the same [51].

There are several theories of PLCs that help us to connect the macroscopic behavior to molecular structures and interactions. The most complete is the statistical mechanical theory originally formulated by Flory in 1956 [18] and then developed further by him, his students, and his collaborators [18,20–22,54].

The Flory theory involves using a lattice. A chain segment can be placed on a lattice site; the solvent molecule has the same dimensions. One assumes that the combinational contribution to the partition function is independent of the orientational contribution. The latter arises from the possible orientations of rigid sequences and from the anisotropic interactions between the segments.

The Flory theory, together with its extentions, makes possible a number of predictions. We know that there are several types of LC phases, classified as nematic, cholesteric, and smectic [55]. The theory predicts conditions necessary for a formation of each of these types of phases in PLCs [56,57]. Moreover, for a ternary system of the kind flexible EP + PLC + solvent one obtains predictions of miscibility gaps in good agreement with experiment [21]. That diagram can be viewed on the Gibbs triangle as an isothermal crosssection. We have homogenous regions close to the triangle tops where one of the components dominates. In a large part of the diagram we have two phases, one PLC–rich and one EP–rich. The theory also predicts *channeling* [21], namely that the LC sequences in PLC chains cause orientation of flexible EP chains between them. This prediction is confirmed by subsequent experimental data, including the P-V-T results for a series of PET/xPHB copolymers with varying x, these in the solid as well as in molten states [58].

Optimization of the alignment process through varying the time of exposition to the field, temperature of the sample, and strength of the field can produce PLC samples with favorable intrinsic order. To see the results of such alignment on mechanical properties, consider a PET/0.6 PHB copolymer. We recall that this blend belongs to longitudinal thermotropic PLCs, the simplest type, containing rodlike mesogens connected parallel to the backbone, see again Section 2.

To measure the change in the material structure the ultrasound critical-angle reflectometry (UCR), a method developed by Antich and co-workers, was used.

Consider the schematic in Figure 15: the transmitted ultrasound beam is reflected off the sample and picked up by the receiver. Measurements are made in the plane defined by the normal to the

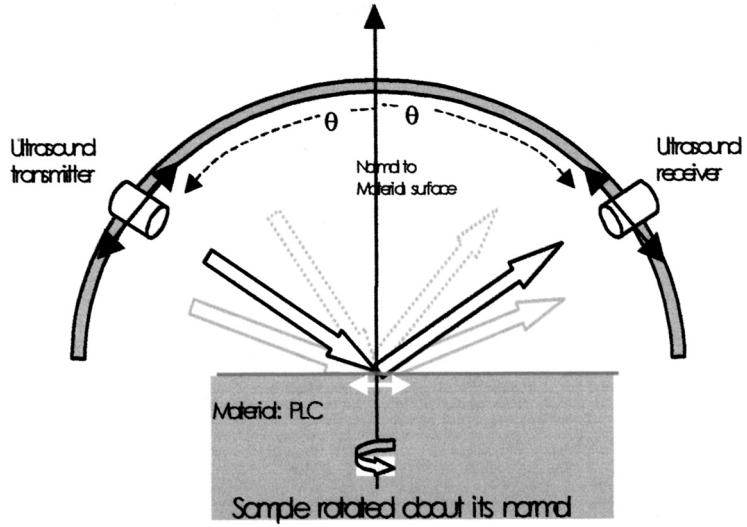

FIGURE 15 Scheme of the UCR.

specimen surface and the incident beam. The transducers move synchronously, maintaining equal angular separation from the normal, collecting the reflected amplitude and phase spectra at various angles of incidence. The incidence angles at which total internal reflection

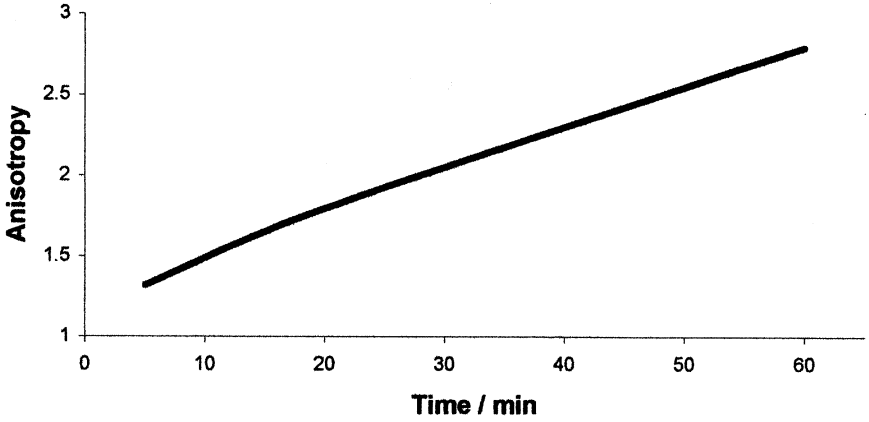

FIGURE 16 Change of anisotropy with time (1.8 B, 280 °C) (parallel to field direction); after [63].

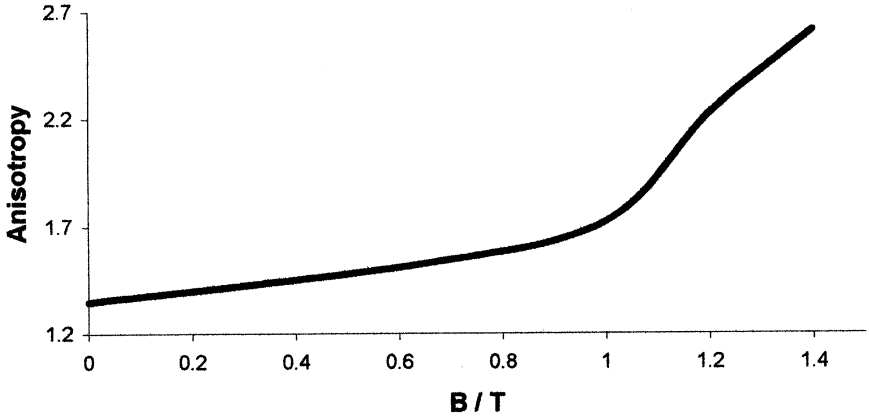

FIGURE 17 Change of anisotropy with magnetic strength (280°C, 30 min) (parallel to field direction); after [63].

occurs are called critical angles; defined from predictable characteristics in the spectra [59], they are used to determine the velocity of pressure and shear waves [60] in the measurement plane in the sample. By rotating the sample about its normal, the measurement plane can be specified at multiple orientations and the variation of pressure and shear velocity with sample orientation can be obtained as desired. The anisotropy of the elastic properties of the material is

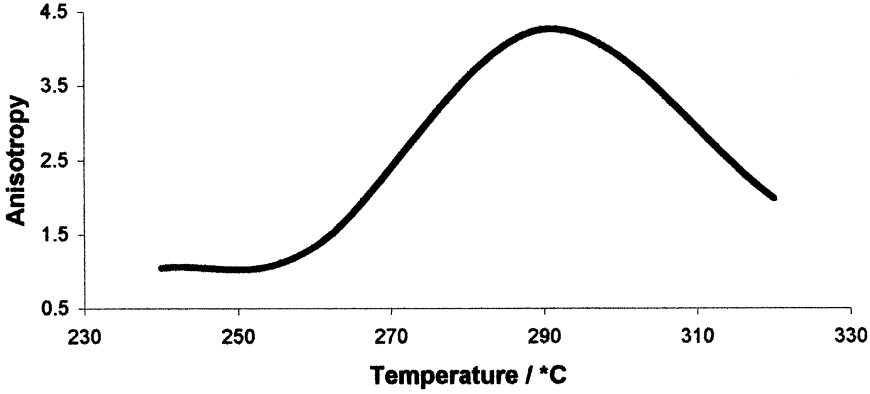

FIGURE 18 Change of anisotropy with increasing temperature (1.8 B, 30 min) (parallel to the field direction); after [63].

calculated as the ratio of maximum velocity to the minimum velocity squared [61,62].

Let us follow the increase in sample alignment as recorded by UCR. Figures 16–18 represent relations between anisotropy and imposed field characteristics obtained by us [63].

In Figure 16 the anisotropy is measured as a function of time τ. Results obtained by exposure to a field of 1.8 T at 280°C are presented. The anisotropy increases with the time of exposure, as expected. We see that the equilibrium state was not reached, even after 60 minutes, when the experiment was terminated.

In Figure 17 we present the anisotropy measured as a function of magnetic induction B by exposure to the field during 30 min at a temperature of 280°C. We see that the anisotropy increases significantly when one imposes a strong field. The Freedericksczz transition is seen clearly. Again, one expects that at sufficiently high field strength a saturation value for anisotropy should be achieved. Here such a value was not found.

To interpret the results of experiments at different temperatures, one should turn to the phase diagram of PET/xPHB copolymers (discussed previously in Section 2). In Figure 18 one can see a rapid increase of anisotropy at temperatures above 250°C. In the phase diagram this is the transition temperature from region X, where the phases present are smectic E (originating from PHB) and the isotropic liquid (originating from PET constituent) to region XI where smectic E and smectic B coexist along with the isotropic liquid. Thus, the creation of the second LC phase strongly increases the orientation. As discussed in [64] by one of us, at least two effects contribute to that result. First, we recall *channeling*—discussed above in the present section—which constitutes the first effect.

Thus, the presence of the smectic B phase apparently increases channeling and subsequent orientation of flexible PET sequences between the LC sequences.

The second effect is the change in materials morphology. The PLC rigid islands are observed to grow significantly until the temperature reaches 320°C [64], when the islands undergo gradual dissolution in the PET–rich phase. Around that temperature, on the phase diagram there is a transition from region XI to XII; in the latter the smectic B phase coexists with the isotropic liquid [13], see again Figure 1. Given this information, we conclude that the growth of island size is the additional creator of orientation, so that the channeling effect is enhanced.

REFERENCES

[1] Travinska, T. V., Lipatov, Y. S., Karabanova, L. V. (1997). *Book of Abstracts*, 5th International Conference on Polymer Characterization, USA, pp. 57.
[2] Deanin, R., Manion, M. (1999). *Compatibilization of Polymer Blends* in *Polymer Blends and Alloys*, eds. Shonanaike, G. O and Simon, G. P., (Marcel Dekker, New York) Part 1.1 pp. 1–22.
[3] Ellis, T. S., (1999). *Interactions and Phase Behavior of Polyester Blend*, in *Polymer Blends and Alloys*, eds. Shonanaike, G. O and Simon, G. P., (Marcel Dekker, New York). Part 1.3, pp. 209–234.
[4] Brostow, W. (1988). *Kunststoffe* **78**: 411.
[5] Brostow, W. (1990). *Polymer* **31**: 979.
[6] Ellis, T. S. (1995). Blending of Nylon in *Nylon Plastic Handbook*, ed. M. I. Kohan, (Munich, Hanser), pp. 268–283.
[7] Ellis, T. S. (1993). *J. Polymer Sci*, *Phys*. **31**: 1109.
[8] Kuhfuss, H. F. and Jackson, W. J., Jr. (1973). U.S. Patent No. 3,778, 410.
[9] Kuhfuss, H. F. and Jackson, W. J., Jr. (1974). U.S. Patent No. 3,804, 805.
[10] Jackson, W. J., Jr. and Kuhfuss, H. F. (1976). *J. Polymer Sci. Chem. Ed*. **14**, 2043.
[11] Jackson, W. J., Jr. (1980). *Brit. Polymer J*. **12**, 154.
[12] Buchner, S., Chen, D., Gherke, R. and Zachman, H. G. (1988). *Mol. Cryst. Liq. Cryst*. **155**: 357.
[13] Brostow, W., Hess, M., and Lopez, B. (1994). *Macromolecules* **27**: 2262.
[14] Brostow, W., Dziemianowicz, T., Romanski, J. and Weber, W. (1988). *Polymer Eng. & Sci*. **28**: 785.
[15] Sun, T. and Porter, R. S. (1990). *Polymer Commun*. **31**: 70.
[16] Kwiatkowski, M. and Hinrichsen, G. (1990). *J. Mater. Sci*. **25**: 1548.
[17] Brostow, W. and Hess, M. (1992). *Mater. Res. Soc. Symp*. **255**: 57.
[18] Flory, P. J. (1956). *Proc. Royal Soc. A*. **234**: 60.
[19] Matheson, R. R., Jr and Flory, P. J. (1981). *Macromolecules* **14**: 954.
[20] Jonah, D. A., Brostow, W. and Hess, M. (1993). *Macromolecules* **26**: 76.
[21] Blonski, S., Brostow, W., Jonah, D. A. and Hess, M. (1993). *Macromolecules* **26**: 84.
[22] Brostow, W. and Walasek, J. (1994). *Macromolecules* **27**: 2923.
[23] Sukhadia, A. M., Done, D. and Baird, D. G. (1990). *Polymer Eng. & Sci*. **30**: 519.
[24] Brostow, W., D'Souza, N. A., Kubat, J. and Maksimov, R. (1999). *Inter. J. Polymer. Mater.* **43**: 233.
[25] Brostow, W., D'Souza, N. A., Kubat, J. and Maksimov, R. (1999). *J. Chem. Phys*. **110**: 9706.
[26] Brostow, W., Hess, M., Lopez, B. and Sterzynski, T. (1996). *Polymer* **37**: 1551.
[27] Lopez, B. (1994). Doctoral Thesis, University of North Texas.
[28] Brostow, W., Sterzynski, T. and Triouleyre, S. (1996). *Polymer* **37**: 1561.
[29] Gaylord, N. G. (1989). *Macromol. Sci*. **A26**: 1211.
[30] Croteau, J. F. and Laivins, G. V. J. (1990). *Appl. Polymer Sci*. **39**: 2377.
[31] Laivins, G. V.(1989). *Macromolecules* **22**: 3974.
[32] Datta, A. and Baird, D. G. (1995). *Polymer* **36**: 505.
[33] Datta, A., Chen, H. H. and Baird, D. G. (1993). *Polymer* **34**: 759.
[34] Brostow, W. (1998). Computer Simulations in *Mechanical and Thermophysical Properties of Polymer Liquid Crystals*, ed. W. Brostow, (Chapman and Hall, New York), Chapter 15, pp. 495–509.
[35] Bratley, P., Fox, B. L. and Schrage, L. E. (1983). *A Guide to Simulation* (Springer-Verlag, New York).
[36] Brostow, W. and Drewniak, M. (1996). *J. Chem. Phys*. **105**: 7135.

[37] Brostow, W., Drewniak, M., and Medvedev, N. N. (1995). *Macromol. Theory & Simul*. **2**: 745.
[38] Metropolis, N. and Ulam, S. (1949). *J. Amer. Statist. Assoc*. **44**: 335.
[39] Alder, B. J. and Wainwright, T. E. (1957). *J. Chem. Phys*. **27**: 1208.
[40] Mom, V. (1981). *J. Comput. Chem*. **2**: 446.
[41] Blonski, S., Brostow, W. and Kubat, J. (1994). *J. Phys. Rev. B* **49**: 6494.
[42] Blonski, S. and Brostow, W. (1991). *J. Chem. Phys*. **95**: 2890.
[43] Menczel, J. and Wunderlich, B. (1980). *J. Polymer Sci. Phys*. **18**: 1433.
[44] Menczel, J. and Wunderlich, B. (1981). *Polymer* **22**: 778.
[45] Meesiri, W., Menczel, J., Gaur, U. and Wunderlich, B. (1982). *J. Polymer Sci. Phys*. **20**: 719.
[46] Brostow, W., Donahue, M., Karashin, C. E. and Simoes, R. (2001). *Mat. Res. Innovat*. **4**: 75.
[47] Brostow, W., Cunha, A. M., Quantanilla, J. and Simoes, R. (2002). *Macromol. Theory & Simul.* **11**: 308.
[48] van Gusteren, W. F. (1988). *Mathematical Frontiers in Computational Chemical Physics* (ed. D. G. Truhlar), (Springer, New York).
[49] Allenand, M. P. and Tidesley, D. J. (1987). *Computer Stimulation of Liquids* (Clarendon Press, Oxford).
[50] Brostow, W. (2000). *The Chain Relaxation Capability.* Chapter 5 in *Performance of Plastics*. (ed. Brostow, W.) Hanser Publishers, Munich, Germany.
[51] Collins, P. (1990) *Liquid Crystals Nature's Delicate Phase of Matter*, (Princeton University Press, Princeton) pp 45–47.
[52] Brostow, W. and Walasek, J. (2000). *Intern. J. Polymer. Mater*. **45**: 169.
[53] Flory, P. J., and Abe, A. (1978). *Macromolecules* **11**: 1119.
[54] Matheson, R. R. (1986). *Macromolecules*, **19**: 1286.
[55] Brostow, W. (1979). *Science of Materials* (Wiley, New York).
[56] Brostow, W. and Walasek, J. (1996). *J. Chem. Phys*. **105**: 4367.
[57] Brostow, W., Hibner, K. and Walasek, J. (1998). *J. Chem. Phys*. **108**: 6484.
[58] Berry, J. M., Brostow, W., Hess, M. and Jacobs, E. G. (1998). *Polymer* **39**: 4081.
[59] Antich, P. and Mehta, S. (1997). *Physics Med. Biol*. **42**: 1763.
[60] Antich, P., et al. (1991). *J. Bone & Min. Res*. **6**: 417.
[61] Mehta, S., Antich, P. and Landis, W. (1999). *Conn. Tissue Res*. **40**: 189.
[62] Mehta, S. (1999) Ultrasound critical angle reflectometry: website (www.swmed.edu/home_pages/ucrlab/) University of Texas Southwestern Medical Center.
[63] Brostow, W., Jaklewicz, M., Mehta, S. and Montemartini, P. (2002). *Mater. Res. Innovat*. **5**: 261.
[64] Brostow, W., Faitelson, E., Kamensky, M., Korkhov, V. and Rodin, Y. (1999). *Polymer* **40**: 1441.